Measuring fast gene dynamics in single cells with time-lapse luminescence microscopy

Anyimilehidi Mazo-Vargas[a,b,c], Heungwon Park[a,b,c,d], Mert Aydin[a,b,c], and Nicolas E. Buchler[a,b,c,d]
[a]Institute for Genome Sciences and Policy, [b]Duke Center for Systems Biology, [c]Department of Biology, and [d]Department of Physics, Duke University, Durham, NC 27710

ABSTRACT **Time-lapse fluorescence microscopy is an important tool for measuring in vivo gene dynamics in single cells. However, fluorescent proteins are limited by slow chromophore maturation times and the cellular autofluorescence or phototoxicity that arises from light excitation. An alternative is luciferase, an enzyme that emits photons and is active upon folding. The photon flux per luciferase is significantly lower than that for fluorescent proteins. Thus time-lapse luminescence microscopy has been successfully used to track gene dynamics only in larger organisms and for slower processes, for which more total photons can be collected in one exposure. Here we tested green, yellow, and red beetle luciferases and optimized substrate conditions for in vivo luminescence. By combining time-lapse luminescence microscopy with a microfluidic device, we tracked the dynamics of cell cycle genes in single yeast with subminute exposure times over many generations. Our method was faster and in cells with much smaller volumes than previous work. Fluorescence of an optimized reporter (Venus) lagged luminescence by 15–20 min, which is consistent with its known rate of chromophore maturation in yeast. Our work demonstrates that luciferases are better than fluorescent proteins at faithfully tracking the underlying gene expression.**

Monitoring Editor
Karsten Weis
ETH Zurich

Received: Jul 7, 2014
Revised: Aug 28, 2014
Accepted: Sep 5, 2014

INTRODUCTION

Time-lapse fluorescence microscopy of genetically encoded fluorescent proteins is the gold standard for measuring in vivo dynamics of gene expression in single cells. However, fluorescence microscopy uses intense light to excite a fluorophore, which can result in high background autofluorescence and phototoxicity in cells. This problem becomes acute when measuring multiple genes (which requires exciting different fluorophores with different wavelengths) on fast time scales (which requires frequent exposure to intense light). For these reasons, time-lapse fluorescence microscopy is typically limited to one or two fluorescent reporters. A further limitation is the slow chromophore maturation of fluorescent proteins, which can introduce a significant time delay between gene expression and measurable change in fluorescence. Fluorescent protein reporters with long maturation times cannot faithfully track gene expression dynamics (Wang *et al.*, 2008; Gedeon and Bokes, 2012)

An alternative is luciferase, an oxidative enzyme that produces photons. Luciferases fold cotranslationally and are enzymatically active upon folding (Frydman *et al.*, 1999). Thus, in contrast to fluorescent proteins, they do not require intense excitation light and do not exhibit maturation delays. Luciferases are an example of convergent evolution because diverse organisms (e.g., beetles, marine invertebrates, bacteria) have independently evolved enzymes to produce light of different colors using unique substrates (e.g., D-luciferin, coelenterazine, and N-decanal; Wilson and Hastings, 1998). Despite this enzymatic diversity, all known luciferases require oxygen to catalyze their substrate into an excited-state product that decays and emits a single photon. The ability to maintain in vivo oxygen and substrate concentrations at high and consistent levels during live-cell time-lapse luminescence microscopy has been a challenge. Another limitation is the number of photons produced per luciferase per second. The maximum catalytic rates of beetle and marine luciferases range from 0.1 to 10 photons/s per luciferase (Branchini *et al.*, 1999; Loening *et al.*, 2006). This is substantially lower than the 1000 photons/s per green fluorescent protein (GFP) at an excitation intensity of 10 W/cm^2 (Garcia-Parajo *et al.*, 2000; Chiu *et al.*, 2001).

This article was published online ahead of print in MBoC in Press (http://www.molbiolcell.org/cgi/doi/10.1091/mbc.E14-07-1187) on September 17, 2014.

Address correspondence to: Nicolas E. Buchler (nicolas.buchler@duke.edu).

Abbreviations used: Ade, adenine; CCD, charge-coupled device; GFP, green fluorescent protein; Leu, leucine; Lys, lysine; Met, methionine; NLS, nuclear localization signal; SCD, synthetic complete dextrose; SLIC, Sequence and Ligation Independent Cloning; yEVenus, yeast-enhanced Venus; YFP, yellow fluorescent protein.

Supplemental Material can be found at:
http://www.molbiolcell.org/content/suppl/2014/09/15/mbc.E14-07-1187v1.DC1.html

Time-lapse luminescence microscopy has been successfully used to measure in vivo gene dynamics in larger organisms (e.g., animals, plants, tissue culture) or for slower processes (e.g., circadian oscillation), for which more total photons per pixel can be collected during one camera exposure (Liu *et al.*, 2007; Nakajima *et al.*, 2010). The state of the art for microbial time-lapse luminescence microscopy measured circadian gene dynamics in single cyanobacteria with a 30-min exposure time (Mihalcescu *et al.*, 2004). To our knowledge, no one has developed methods of microbial time-lapse luminescence microscopy that measure in vivo gene dynamics for extended periods of time with subminute resolution (e.g., cell cycle).

Commercial time-lapse microscopes and sensitive charge-coupled device (CCD) cameras have greatly improved over the last decade and are routinely used by biologists. Thus we sought to improve in vivo luciferase enzymatic yield (photons per second) rather than photon detection. We developed a method for live-cell time-lapse luminescence microscopy that can measure subminute gene dynamics in budding yeast at single-cell resolution. This was achieved by optimizing D-luciferin delivery across the lipid bilayer, using microfluidics to trap cells and maintain substrates at saturating concentrations during imaging, and integrating multiple copies of luciferase genes into the yeast genome.

RESULTS

We first designed and constructed green (GrLuc), yellow (YeLuc), and red (RdLuc) luciferase derived from beetles (Viviani *et al.*, 1999a,b; Fujii *et al.*, 2007). We fused an N-terminal nuclear-localization signal (NLS) to concentrate these luciferases into a smaller volume and spread the light signal across fewer pixels (Figure 1A). For comparison, we also tested commercial beetle luciferases (CBG99, CBR, FLuc) and a new marine luciferase (NLuc; Hall *et al.*, 2012) from Promega (Madison, WI; Figure 1B). Each luciferase reporter was regulated by a methionine-repressible promoter (*MET17*) and integrated into the yeast genome either in single copy or multiple copies; see *Materials and Methods*. We measured the emission spectrum of our designed luciferases to confirm that they were consistent with their expected color; see Supplemental Figure S1.

We then used a 96-well plate bulk assay with a Wallac Victor 3 luminometer (PerkinElmer-Cetus, Waltham, MA) to optimize conditions (substrates, pH) for in vivo yeast luminescence. Beetle luciferases require D-luciferin, ATP, and oxygen as substrates, whereas NLuc only requires furimazine (a coelenterazine analogue) and oxygen. We expected log-phase cells to maintain their ATP at high concentrations. However, in vivo oxygen, D-luciferin, and furimazine could be limiting because they must diffuse across the lipid bilayer from the external medium (Wood and DeLuca, 1987; Vieites *et al.*, 1994). We determined that 200 μM D-luciferin and 50 μM furimazine were saturating for in vivo luminescence (Figure 2A). We further boosted the in vivo luminescence of beetle luciferases ~30-fold by lowering the pH of the growth medium (Figure 2B). The luminescence increased because of the low extracellular pH, which reduced the charge of D-luciferin ($pK_a = 2.9$) and improved its diffusion across the lipid bilayer (Wood and DeLuca, 1987; Vieites *et al.*, 1994). We verified that our yeast strains grew well at lower pH (3.8) and that the luciferases were not cytotoxic at high copy number (Figure 2C). The only exception is NLuc, which was already cytotoxic as a single-copy integrant (Figure 2C).

We also compared the relative brightness of different luciferases. To this end, we integrated a single gene copy of each luciferase into the same target locus. Our beetle luciferases GrLuc and YeLuc were ~10-fold brighter than RdLuc (Figure 3A). This same color relationship persists for Promega beetle luciferases CBG99 (green), FLuc

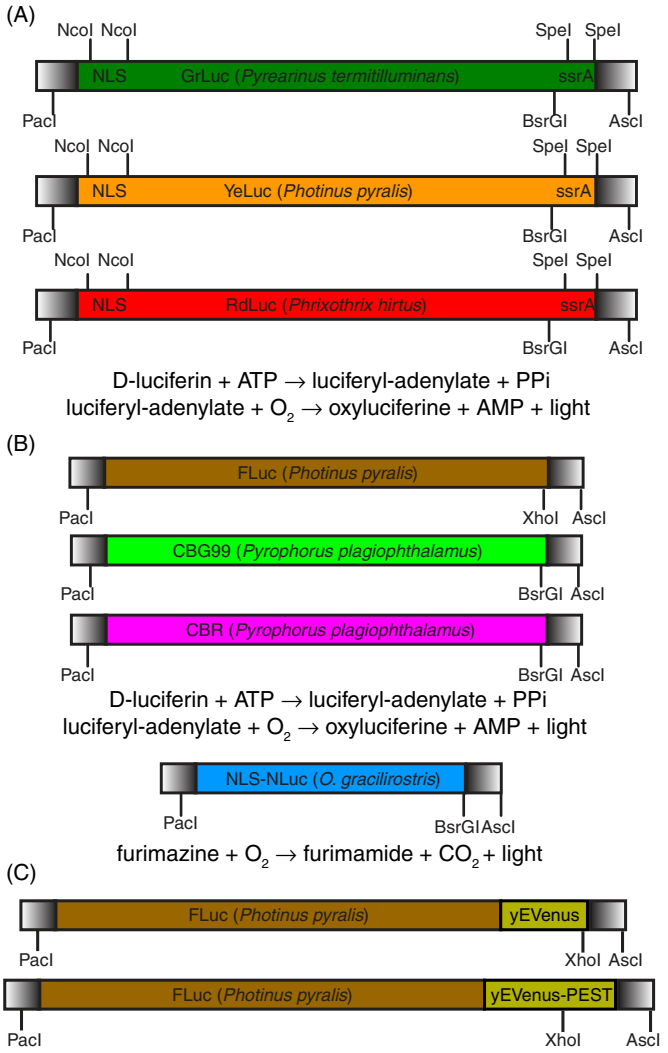

FIGURE 1: Construction and design of multicolor luciferases. (A) We used gene synthesis (DNA 2.0, Menlo Park, CA) to build beetle luciferases—green from *P. termitilluminans* (Viviani *et al.*, 1999b), yellow from *P. pyralis* (Fujii *et al.*, 2007), and red from *P. hirtus* (Viviani *et al.*, 1999a)—for expression in budding yeast. Beetle luciferase is an enzyme that catalyzes a two-step reaction that requires both ATP and O_2 in addition to D-luciferin substrate. An N-terminal SV40 NLS was added between *NcoI*–*NcoI* to concentrate luciferase into the nucleus and improve signal-to-background ratio. The C-terminal SKL peroxisomal targeting motif (Leskinen *et al.*, 2003) was removed and replaced by an ssrA degron between *SpeI*–*SpeI* for future use in an engineered ClpXP yeast strain (Grilly *et al.*, 2007). The ClpXP strain has LacI-regulated expression of ClpX and ClpP, two subunits of a bacterial proteasome that recognizes a short amino acid sequence, ssrA. Any yeast protein in the engineered ClpXP strain that is fused to an ssrA tag will be conditionally degraded by the addition of isopropyl-β-D-thiogalactoside. (B) For comparison, we tested Promega CBG99 (green) and CBR (red) from *P. plagiophthalamus* and FLuc (yellow) from *P. pyralis*. We also tested Promega NLuc (blue), which is a bright marine luciferase that requires only O_2 and furimazine (a coelenterazine analogue; Hall *et al.*, 2012). Blue marine luciferases do not require ATP. All of these gene constructs were built to be modular and backward compatible with popular yeast enhanced fluorescent proteins (*PacI*-*AscI*; Sheff and Thorn, 2004) and yeast PEST degron (*XhoI*/*BsrGI*-*AscI*) derived from *CLN2* gene (Mateus and Avery, 2000). (C) We built FLuc-yEVenus and FLuc-yEVenus-PEST fusion proteins to compare time-lapse luminescence and fluorescence microscopy directly.

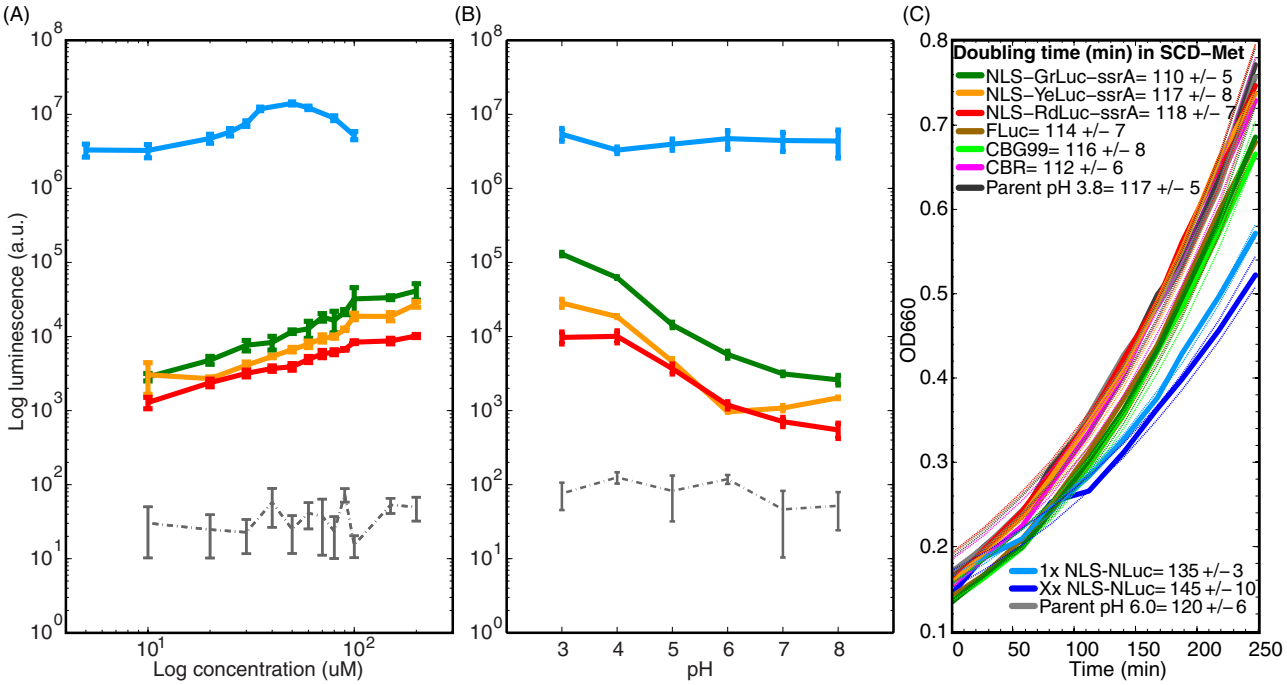

FIGURE 2: Optimization of pH and substrate concentration in the extracellular medium. We used multicopy strains AMV104, AMV68, AMV69, AMV45, AMV152, AMV151, AMV16, and AMV41, which have a *MET17* promoter driving different luciferase reporters; see Table 3. We also included the parental strain (MMY116-2C) as a negative control. Strains were induced overnight and diluted into fresh medium in the morning. Cell cultures were then grown at 30°C to $OD_{660} \approx 0.2$ before starting measurements. Growth medium was synthetic complete methionine drop-out medium with 2% D-glucose (SCD–Met). The bulk luminescence was measured using a 96-well plate assay with a Wallac Victor 3 plate reader. Error bars represent the SD of three technical replicates. (A) We varied the D-luciferin and furimazine concentrations at constant pH values (3.8 and 6.0, respectively). (B) We varied the pH of the growth medium at constant D-luciferin (100 μM) or furimazine (20 μM) concentrations. On the basis of these results, we fixed the pH (3.8), D-luciferin (100 μM), and furimazine (20 μM) for all subsequent luminescence experiments. (C) We measured OD_{660} every 30 min with a spectrophotometer to quantify strain growth rates in SCD-Met at 30°C. Thin, dotted lines are the 95% confidence interval of the best exponential fit. Both single-copy and multicopy Nluc exhibited slower growth rates than the parental strain.

(yellow), and CBR (red). All of the commercial luciferases were at least ~10-fold brighter (Figure 3A) than our designed luciferases. NLuc was the brightest. Unfortunately, furimazine was insoluble in aqueous solution and precipitated out, which made NLuc incompatible with long-term, live-cell time-lapse luminescence microscopy.

We screened all multicopy transformants using a 96-well plate luminescence assay and selected the "brightest" strains (Figure 3B) for time-lapse luminescence microscopy. The variability in luminescence between transformants arises from unequal copy number integration in chromosomal loci due to homologous ends-in recombination. Time-lapse luminescence microscopy using standard, agarose pad methods initially exhibited bright luminescence signal. However, the signal disappeared within 15 min. We reasoned that luciferase substrates (D-luciferin, oxygen) were being depleted. Thus we combined a CellAsic microfluidic device (EMD Millipore, Billerica, MA) with time-lapse luminescence microscopy. The microfluidic device trapped yeast cells and maintained growth medium at constant levels through perfusion. The medium exchange time was <1 min, and cells were unable to deplete their substrates. With microfluidics, we consistently measured in vivo gene expression dynamics with subminute time resolution for >12 h (Figure 4). We only stopped time lapse because the yeast microcolony extended beyond the field of view. We further validated our method by benchmarking and quantifying gene induction and repression dynamics of many green, yellow, and red luciferase reporters for several metabolite-repressed yeast promoters (*MET17*, *LEU1*, *ADE17*, *LYS9*); see Supplemental Figures S2–S4 and Supplemental Table S1.

To compare luciferase and fluorescent protein reporters directly, we used both time-lapse luminescence and fluorescence microscopy to measure gene induction and repression dynamics of a FLuc-yEVenus-PEST fusion (Figure 1C) regulated by the *LEU1* promoter (Figure 4). We chose yEVenus-PEST because it is a fast-maturing, destabilized yellow fluorescent protein (YFP) commonly used to measure yeast cell cycle dynamics (Skotheim *et al.*, 2008). Our results showed that the fluorescence kinetics of FLuc-yEVenus-PEST during induction and repression are consistently slower and delayed compared with luminescence. The slow kinetics is worse if FLuc-yEVenus is not destabilized with a PEST degron; see Supplemental Figure S5 and Supplemental Table S1. We obtained identical results with FLuc-yEVenus and FLuc-yEVenus-PEST fusions regulated by the *MET17* promoter; see Supplemental Figure S6 and Supplemental Table S1.

These results suggested that our luciferase should more faithfully track cell-cycle oscillations than fluorescence reporters. To this end, we expressed FLuc-yEVenus-PEST under the transcriptional control of two different yeast cell cycle promoters, *SIC1* and *RNR1*. We successfully tracked cell cycle luciferase dynamics with subminute resolution (Figure 5). SIC1 transcripts are known to peak at the M/G1 border near cytokinesis, whereas *RNR1* transcripts peak at the G1/S border (Spellman *et al.*, 1998). Our data showed that the luminescence of *SIC1pr-FLuc-yEVenus-PEST* peaks on average 13 min

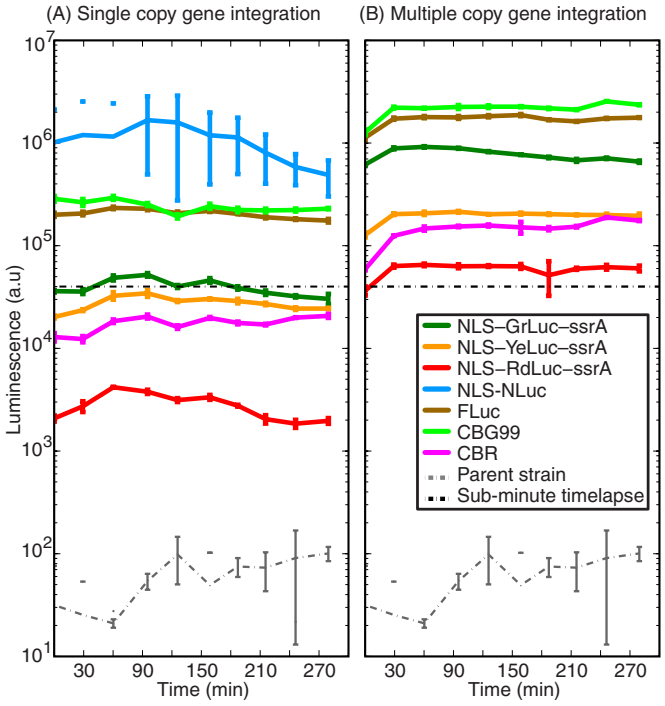

FIGURE 3: Luminescence output of different multicolor luciferases integrated in yeast chromosome as (A) a single copy or (B) multiple copies. Single-copy strains were AMV70, AMV72, AMV71, AMV54, AMV152-13, AMV151-18, and AMV16, and "bright," multicopy strains were AMV104, AMV68, AMV69, AMV45, AMV152-03, and AMV151-08; see Table 3. All strains have a *MET17* promoter driving different luciferase reporters. We also included the parental strain (MMY116-2C) as a negative control. We used a 96-well plate assay, and error bars represent the SD of three technical replicates. At time t = 0 min, 100 µl of log-phase (OD_{660} = 0.1) yeast pregrown at 30°C in SCD–Met were inoculated in fresh, identical medium with 100 µM D-luciferin at pH 3.8 or 20 µM furimazine at pH 6.0. Time-lapse luminescence microscopy at subminute time resolution was successful for those strains above the horizontal, dashed line at 4×10^4 luminescence units. With the exception of CBR, commercial luciferases are bright enough at single copy for subminute time-lapse luminescence microscopy in budding yeast.

before budding, whereas fluorescence peaks 6 min after budding. The luminescence of *RNR1pr-FLuc-yEVenus-PEST* peaks on average 7 min before budding, and fluorescence peaks 11 min after budding. Thus fluorescence lagged the luminescence signal by 15–20 min. This delay was identical to the measured in vivo chromophore maturation delay of yEVenus-PEST (Charvin *et al*., 2008). To verify that our protein fusion was not interfering with yEVenus folding and/or maturation, we built strains with either yEVenus-PEST or FLuc under the control of *SIC1* or *RNR1* promoter, respectively. Fluorescence of yEVenus-PEST alone continued to exhibit a 15–20 min delay when compared with luminescence of FLuc (Supplemental Figure S7). A two-sample Student's *t* test of our fluorescence peak and budding data shows no significant statistical difference between FLuc-yEVenus-PEST (Figure 5) and yEVenus-PEST (Supplemental Figure S7) with either *SIC1* or *RNR1* promoter; see Supplemental Table S2 for a complete statistical analysis. The same is true for luminescence peak and budding data between FLuc-yEVenus-PEST and FLuc. Supplemental Table S2 also shows that PEST has no significant effect on the timing of peak signal and budding. We conclude that FLuc-yEVenus-PEST fusion does not significantly affect the timing of either FLuc luminescence or yEVenus fluorescence.

DISCUSSION

Here we optimized luminescence microscopy to measure in vivo gene dynamics (e.g., cell cycle) in yeast cells with subminute resolution. The temporal resolution was ~4 times faster and the cellular volumes were ~20 times smaller than previous methods with beetle luciferases (Supplemental Table S3). Our protocol now adds time-lapse luminescence microscopy to the microbiologist's toolbox for measuring fast gene dynamics with a beetle luciferase. Time-lapse luminescence can be used alone (if phototoxicity and/or chromophore maturation is a problem) or in conjunction with time-lapse fluorescence microscopy (if more gene reporters are needed). Successful time-lapse luminescence only required a dark room, a sensitive electron-multiplying (EM) CCD camera, and a microfluidic device to prevent depletion of critical luciferase substrates (e.g., D-luciferin, oxygen). All of this equipment is commercially available and compatible with standard time-lapse fluorescence microscopes. We did not measure dynamics of several genes simultaneously using our multicolor luciferases, but luminescence multiplexing can be done in batch culture (Nakajima *et al*., 2005) and in single cells (Kwon *et al*., 2010) with filters and spectral unmixing.

Our method was developed to study fast transcriptional dynamics. However, luciferases can be fused to proteins to study localization and protein–protein interactions via split luciferases (Ozawa *et al*., 2001; Luker *et al*., 2004; Malleshaiah *et al*., 2010) or bioluminescence resonance energy transfer (Xu *et al*., 1999). If protein localization or transport is fast, the ~1-min exposure time required with a beetle luciferase fusion cannot provide the same spatial resolution as fluorescent proteins. Directed evolution and rational design of blue marine luciferases (e.g., NanoLantern, NLuc) have improved the photon flux ~10- to 100-fold (Hoshino *et al*., 2007; Hall *et al*., 2012). For example, NanoLantern was able to measure protein localization and transport in mammalian cells (Saito *et al*., 2012). Unfortunately, in our hands, NLuc (a blue marine luciferase) was cytotoxic, and furimazine (a derivative of coelenterazine substrate) was insoluble in the microfluidic device. As conditions continue to be improved for in vivo luminescence, luciferases should eventually exhibit all the benefits of fluorescence proteins without the drawbacks. This will also require co-optimizing substrates to be water soluble and diffusible across the lipid bilayer.

MATERIALS AND METHODS

Plasmid construction

Luciferase sequences from larval click beetle (*Pyrearinus termitilluminans*; GrLuc, green), firefly (*Photinus pyralis*; YeLuc, yellow), and railroad worm (*Phrixothrix hirtus*; RdLuc, red) were obtained from GenBank (AF116843, AB261988, AF139645; Viviani *et al*., 1999a,b; Fujii *et al*., 2007). Restriction enzyme cut sites, an N-terminal SV40 NLS, and an ssrA degron tag were added to the sequence. The designed DNA sequence was de novo synthesized by DNA 2.0 (Figure 1) into their pJ204 vector. Optimized luciferases from click beetle, *Pyrophorus plagiophthalamus* (pCBG99, green; and pCBR, red), and deep-sea shrimp, *Oplophorus gracilirostris*, were obtained from Promega. The plasmid pRS303d-KAN-GAL1pr-Luc (A4V) (Robertson *et al*., 2008), which contains the optimized firefly (*P. pyralis*) luciferase from pGL3-Basic vector (Promega), was a gift from the Carl Johnson laboratory at Vanderbilt University (Nashville, TN).

We first built the *MET17* promoter (also known as *MET25*) driving each of the luciferase genes. Parental p406-MET17pr-yEVenus vector was digested with *Pac*I-*Asc*I, and the reporter gene (yEVenus)

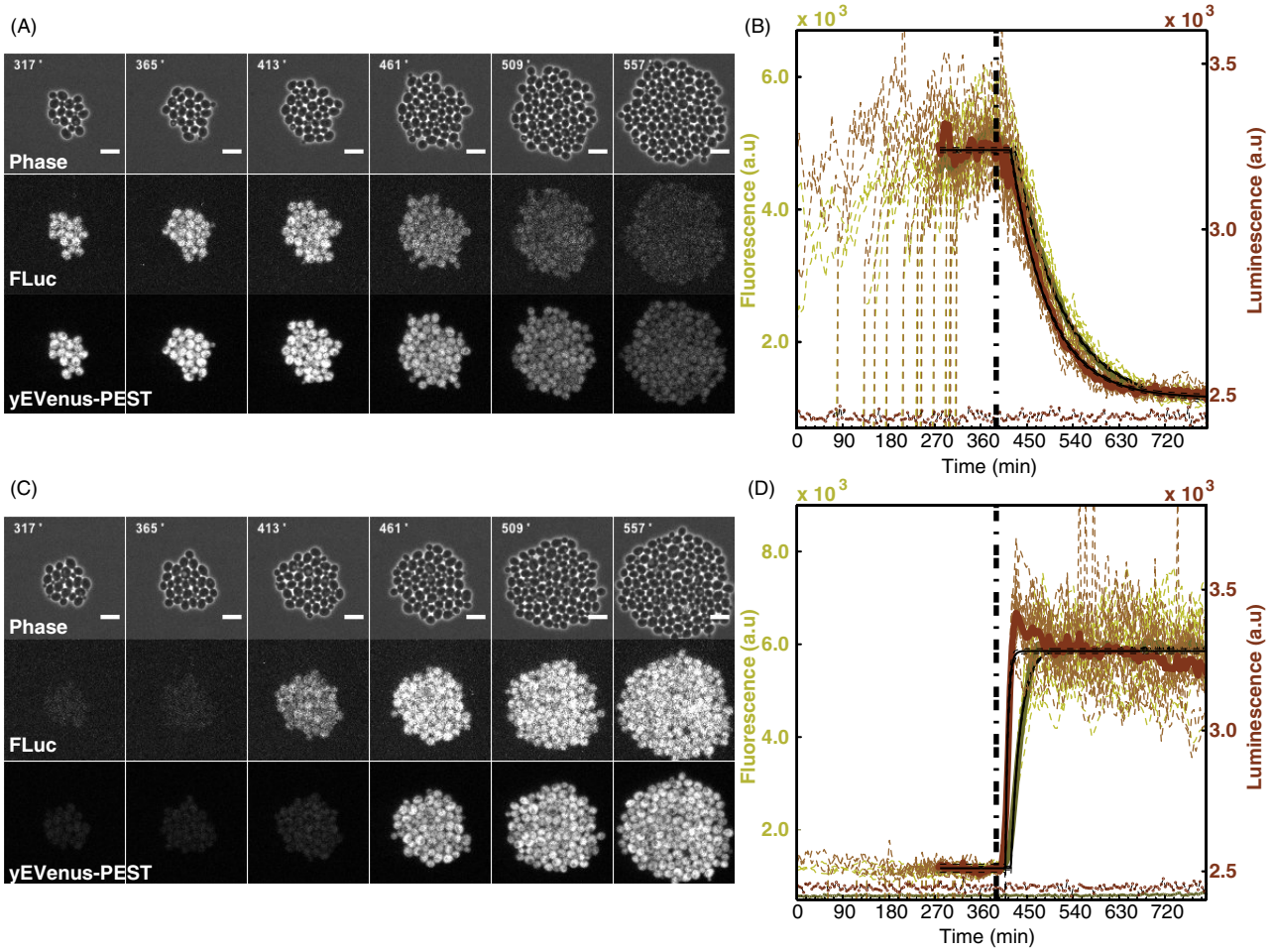

FIGURE 4: Fast-time-lapse luminescence microscopy in budding yeast. Montage of *LEU1pr-FLuc-yEVenus-PEST* switching between leucine repression and induction. Our multicopy strain AMV167 was grown at 30°C on a CellAsic microfluidic device that was mounted on a DeltaVision microscope (Applied Precision, Issaquah, WA) within an incubation chamber. We imaged cells every 4 min. To capture full luminescence, each image is a sum projection of five *z*-stacks separated by 0.4 µm, with 10-s exposures for each stack for a subminute total. We also acquired a 2-ms fluorescence image, followed by a 7-ms phase image for image segmentation. The difference in exposure times indicates that yEVenus emits ~10^4-fold more photons per second than FLuc, which is consistent with known photon flux outputs of fluorescent proteins and luciferases. (A) Previously induced cells were repressed during the switch from SCD-Leu to SCD+Leu medium at 390 min (vertical line in B). (B) Single-cell luminescence and fluorescence traces of repression ($n = 16$ cells). Image segmentation was done with CellStat program (Kvarnström *et al.*, 2008). Rapid increases in signal are the new buds identified and tracked by the segmentation program. Best fit of a mathematical model of gene repression with delay to average luminescence signal (dark brown) and average fluorescence signal (dark green) is shown in black; see *Materials and Methods* and Supplemental Table S1 for details. Thin, black dotted lines are the 95% confidence interval of the best fit curve. The luminescence background is set by EMCCD camera noise, whereas fluorescence background is set by cellular autofluorescence. (C) Previously repressed cells were induced during the switch from SCD+Leu to SCD-Leu medium at 390 min (vertical line in D). (D) Single cell luminescence and fluorescence traces of induction ($n = 18$ cells). Scale bar, 10 µm.

was replaced with a *Pac*I-*Asc*I–digested *luciferase* insert (GrLuc, YeLuc, or RdLuc from pJ204-NLS-*luciferase*-ssrA). In the case of commercial luciferases, the insert genes were amplified from the original vectors (see oligos in Tables 1 and 2). Most of the forward oligos contained a *Pac*I site, whereas the reverse oligos had *Asc*I and *BsrG*I or *Xho*I sites (Figure 1 and Table 1). The resulting PCR product was then digested and ligated to parental p406-MET17pr-yEVenus vector that had been digested with *Pac*I-*Asc*I (Table 2) or integrating using the Sequence and Ligation Independent Cloning (SLIC) method. The "disintegrator" plasmids were built by cutting luciferase inserts and pIS385-MET17pr parental vectors with *Pac*I-*Asc*I, followed by ligation to create pIS385-MET17pr-*luciferases*.

All remaining plasmids with LEU1, ADE17, LYS9, SIC1, and RNR1 promoters were created either by swapping promoters (using *Sac*I-*Pac*I) or by swapping luciferases (using *Pac*I-*Asc*I).

We created a luciferase and fluorescent protein fusion by inserting the yEVenus gene, amplified from p406-MET17pr-yEVenus (see oligos in Table 1), into digested *Xho*I-*Asc*I p406-MET17pr-FLuc using the SLIC method. PEST degron was extracted from p406-MET17pr-FLuc-PEST by *Xho*I-*Asc*I digest and then ligated to *Xho*I-*Asc*I–digested p406-MET17pr-FLuc-yEVenus. The resulting cassette was then inserted after *LEU1*, *SIC1*, and *RNR1* promoters using *Pac*I-*Asc*I cut sites. All plasmids were verified by analytical restriction digest and fragment analysis by 3730xl DNA Analyzer

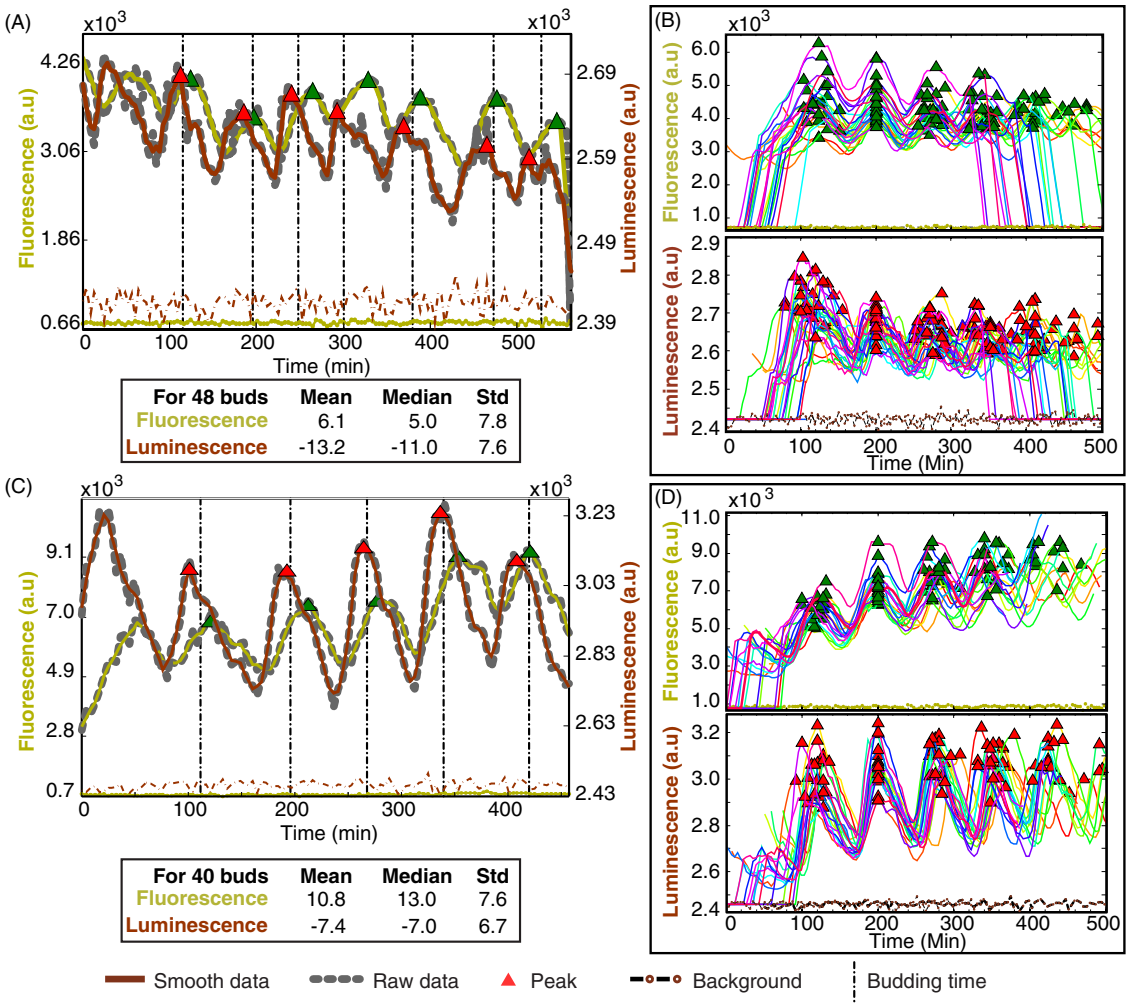

FIGURE 5: Time-lapse luminescence microscopy of cell-cycle dynamics. Single-cell time-lapse luminescence and fluorescence microscopy of multicopy strains AMV163 and AMV165 with (A, B) *SIC1pr-FLuc-yEVenus-PEST* and (C, D) *RNR1pr-FLuc-yEVenus-PEST*, respectively. Filming and image segmentation were identical to Figure 4, except that each luminescence *z*-stack was 12 s. (A) A representative *SIC1pr-FLuc-yEVenus-PEST* and (C) *RNR1pr-FLuc-yEVenus-PEST* time course. The raw, noisy luminescence and fluorescence were smoothed with a Savitzky–Golay filter (with a span of eight data points and one polynomial degree) to reliably detect peak *SIC1* or *RNR1* expression. The vertical, dashed lines in individual traces correspond to budding, a visible cell cycle event. Statistical differences in timing between budding and peak times are reported in tables beneath the figures. The yeast cell division cycle exhibits significant variability in amplitude and period, a feature that leads to loss of synchrony in a population of cells (Di Talia *et al.*, 2007). This loss of synchrony is easily observed when we align different single-cell traces of (B) *SIC1pr-FLuc-yEVenus-PEST* and (D) *RNR1pr-FLuc-yEVenus-PEST* to their second peaks. We align to the second peak because daughter cells are known to have large, variable delays in their first cell cycle (Di Talia *et al.*, 2009).

(Life Technology, Grand Island, NY). Most plasmids in Table 2 are available from Addgene (Cambridge, MA).

Strain construction

Standard methods were used for bacterial and yeast transformations. All yeast strains in Table 3 were derived from MMY116-2C, which is the W303 laboratory strain in which the *ade2-1* mutation was restored to *ADE2*. Multicopy strains in Table 3 were created using homologous ends-in recombination at the *URA3* or LEU2 locus after plasmid linearization by *Stu*I or *Afl*II digestion, respectively. A consequence of ends-in homologous recombination is that different transformants will have different numbers of plasmid copies integrated into their target locus (Orr-Weaver *et al.*, 1981). Most single-copy strains in Table 3 were created using a URA3 pop-in/pop-out "disintegrator plasmid" (Sadowski *et al.*, 2007). Briefly, the luciferase gene and *URA3* are integrated via homologous ends-in recombination into the *LYS2* locus after *Nru*I digestion of plasmids. Subsequent selection for *URA3* pop out results in a single gene integration of luciferase in disrupted *LYS2* locus (*lys2Δ*). Single-copy integration was confirmed by PCR. All strains in Table 3 are available upon request.

Ninety-six–well plate luminescence assay

A Wallac Victor 3 plate reader was used to measure luminescence intensity (Figures 2 and 3). Yeast strains were grown overnight to reach $OD_{660} \approx 0.2$. Our growth medium was SCD–Met at pH 3.8 for beetle luciferases and pH 6.0 for NLuc. The samples were then diluted to $OD_{660} \approx 0.1$ and loaded in a 96-well black assay plate (nontreated) with flat, clear bottom. At the beginning of the time course, 100 μM beetle luciferin or 20 μM furimazine was added to the cell cultures. All cultures were grown in a 30°C incubator, and

Target sequence	Oligo name	Oligo sequence 5′ → 3′	Cut sites
FLuc gene from pRS303d-KAN-GAL1pr-FLuc(A4V) plasmid; ligation using SLIC protocol	SLIC_FLuc_FWD	ATTACCCCCATCCATACTCTAGAACTAGTGGATCCCCCG-GGTTAATTAACATGGAAGACGTCAAAAACAT	*Pac*I
	SLIC_FLuc_REV	TCATAAATCATAAGAAATTCGCTTATTTAGAAGTGGCGCGC-CTTATTCTCGAGACACGGCGATCTTTCCGC	*Asc*I *Xho*I
NLuc gene from pNL1.1 plasmid	PacI_NLS_NLuc	CTCTTAATTAACACCATGGCACCACCAAAGAAAAAGAG-AAAAGTAGCCATGGTCTTCACACTCGAAGAT	*Pac*I
	AscI_BsrGI_NLuc	AGTGGCGCGCCTTATTTGTACAACGCCAGAATGCGTTCG-CACA	*Asc*I *BsrG*I
yEVenus gene from p406-MET-17pr-yEVenus plasmid; ligation using SLIC protocol	SLIC_FLuc_YFP_fwd	AAGAAGGGCGGAAAGATCGCCGTGGGTGGGGGATCAAT-GTCTAAAGGTGAAGAATTATTC	
	SLIC_FLuc_YFP_rev	AGAAATTCGCTTATTTAGAAGTGGCGCGCCTTATTCTCGA-GATTCATCAATACCATGGGT	*Asc*I *Xho*I
CBG99 gene from CBG99-control plasmid	MET25_PacI_CB_F	CATACTCTAGAACTAGTGGATCCCCCGGGTTAATTAACCAT-GGTGAAGCGTGAGAAAAATGTC	*Pac*I
	Adh_BsrGI_CBG99_R	AATTCGCTTATTTAGAAGTGGCGCGCCTTATTTGTACAAAC-CGCCGGCCTTCTCCAACAA	*Asc*I *BsrG*I
CBR gene from CBR-control plasmid	MET25_PacI_CB_F	CATACTCTAGAACTAGTGGATCCCCCGGGTTAATTAACCAT-GGTGAAGCGTGAGAAAAATGTC	*Pac*I
	Adh_BsrGI_CBR_R	AATTCGCTTATTTAGAAGTGGCGCGCCTTATTTGTACAAAC-CGCCGGCCTTCACCAACAA	*Asc*I *BsrG*I

SLIC, Sequence- and ligation-independent cloning.

TABLE 1: Oligos.

before each measurement, plates were vortexed for 30 s to resuspend and oxygenate the cell cultures. Luminescence intensity in each well was measured over a 0.5-s exposure time, and samples were spread along the plate in a chess pattern to minimize light leakage from well to well.

Time-lapse luminescence microscopy

The brightest multicopy strain of each luciferase (Figure 3B) was grown in culture tubes overnight in a 30°C incubator to reach $OD_{660} \approx 0.1–0.2$. Metabolite-repressed promoter strains were pregrown in dropout medium to induce (SCD-Metabolite) or in synthetic complete medium to repress (SCD) luciferases. The CellAsic microfluidic chamber has a ceiling height of 4 µm, which is the dimension of haploid yeast. However, yeast cells are naturally flocculent and clump during pregrowth. Thus we sonicated the yeast in a Bioruptor UCD-200 sonicator (Diagenode, Denville, NJ) for 30 s at medium intensity to obtain single-cell suspensions before loading them onto microfluidic plates (CellAsic). Media distribution was controlled by ONIX microfluidic perfusion platform, which provides a well-oxygenated environment. Bioluminescence imaging of yeast cells was performed with a DV Elite microscope equipped with UltimateFocus, an Evolve EMCCD camera (Photometrics, Tucson, AZ), and a 60×/1.25 numerical aperture phase-contrast oil objective lens. Cells were grown at 30°C in complete (SCD) or dropout medium (SCD–Met, SCD–Ade, SCD–Lys, SCD–Leu) at pH 3.8. The medium was supplemented with 200 µM beetle D-luciferin. We imaged cells every 4 min. To improve signal-to-noise ratios, we used 2 × 2 binning (256 × 256 pixels) and a camera gain of 55 with a transfer speed of 5000. The microscope was in an isolated, dark room with a floor-to-ceiling curtain. All light sources in the microscope, computer, and other equipment in the room were wrapped with foil paper and dark tape. We blocked all excitation light, and we removed the emission filters to maximize light transmission. We also modified our time-lapse macro to turn off the UltimateFocus laser every time we did a luminescence exposure.

Time-lapse files with raw luminescence data were preprocessed in Fiji (Schindelin *et al.*, 2012) in the following order: 1) remove bright spot artifacts (i.e., hot pixels), with Remove Outliers function (threshold 1000; 20-pixel radius) for each *z*-slice, 2) use Sum Slices projection under *Z Project* menu, and 3) save integrated *z*-stack in tiff format. Phase-contrast images were imported into CellStat (a MATLAB plug-in; Kvarnström *et al.*, 2008) to segment and track yeast cells over time. Each cell contour over time was verified manually and refined when needed. To retrieve the total luminescence and fluorescence for each cell, the preprocessed luminescence files were imported into CellStat and merged with phase-contrast image contours. Time-course data and statistics were retrieved using the Highest method from CellStat.

Fitting a simple model of gene expression to luminescence data

We developed a quantitative model of gene expression to objectively compare different luciferases as transcriptional reporters. The simplest is a binary model of transcription, which assumes that upon induction or repression, the gene expression output jumps between two synthesis rates. The approach to steady state is dictated by the degradation time scale (τ), which could be luciferase inactivation, degradation, and/or dilution through cell growth. To account for delays due to transcription, mRNA processing, translation, folding, or maturation of either luciferase or fluorescent protein, we included an explicit delay term (δ).

Plasmid name	Parental vector	Final plasmid gene	Yeast selectable marker(s)
pNB774	pJ204-*NLS-GrLuc-ssrA*	*NLS-GrLuc-ssrA* (from DNA 2.0)	–
pNB775	pJ204-*NLS-YeLuc-ssrA*	*NLS-YeLuc-ssrA* (from DNA 2.0)	–
pNB776	pJ204-*NLS-RdLuc-ssrA*	*NLS-RdLuc-ssrA* (from DNA 2.0)	–
pNB329	pNL1.1	*NLuc*	–
pNB591	pRS303d-KAN-GAL1pr-Luc (A4V)	*FLuc*	kanMX
pNB770	CBR-control	*CBR*	–
pNB771	CBG99-control	*CBG99*	–
pNB689	p406-MET17pr-yEVenus	*MET17pr-NLS-GrLuc-ssrA*	URA3
pNB690	p406-MET17pr-yEVenus	*MET17pr-NLS-YeLuc-ssrA*	URA3
pNB691	p406-MET17pr-yEVenus	*MET17pr-NLS-RdLuc-ssrA*	URA3
pNB649	p406-MET17pr-yEVenus	*MET17pr-FLuc*[a]	URA3
pNB768	p406-MET17pr-yEVenus	*MET17pr-CBG99*[a]	URA3
pNB769	p406-MET17pr-yEVenus	*MET17pr-CBR*[a]	URA3
pNB648	p406-MET17pr-yEVenus	*MET17pr-NLS-NLuc*	URA3
pNB655	p406-MET17pr-FLuc	*MET17pr-FLuc-yEVenus*[a]	URA3
pNB682	p406-MET17pr-FLuc-yEVenus	*MET17pr-FLuc-yEVenus-PEST*	URA3
pNB695	pIS385-MET17pr-yELucYellow	*MET17pr–NLS–GrLuc–ssrA*	URA3/LYS2
pNB693	pIS385-MET17pr-yELucYellow	*MET17pr-NLS-YeLuc-ssrA*	URA3/LYS2
pNB697	pIS385-MET17pr-yELucYellow	*MET17pr-NLS-RdLuc-ssrA*	URA3/LYS2
pNB660	pIS385-MET17pr-yELucYellow	*MET17pr-FLuc*	URA3/LYS2
pNB330	pIS385-MET17pr-yELucGreen	*MET17pr-NLS-NLuc*[a]	URA3/LYS2
pNB753	p406-GAL1pr-NLS-GrLuc-ssrA	*LEU1pr-NLS-GrLuc-ssrA*	URA3
pNB762	p406-MET17pr-FLuc	*LEU1pr-FLuc*	URA3
pNB786	p406-LEU1pr-NLS-YeLuc-ssrA	*LEU1pr-FLuc-yEVenus*	URA3
pNB787	p406-LEU1pr-NLS-YeLuc-ssrA	*LEU1pr-FLuc-yEVenus-PEST*	URA3
pNB777	p406-LEU1pr-NLS-YeLuc-ssrA	*LEU1pr-CBR*	URA3
pNB778	p406-LEU1pr-NLS-YeLuc-ssrA	*LEU1pr-CBG99*	URA3
pNB752	p406-GAL1pr-NLS-GrLuc-ssrA	*ADE17pr-NLS-GrLuc-ssrA*	URA3
pNB761	p406-MET17pr-FLuc	*ADE17pr-FLuc*	URA3
pNB758	p406-GAL1pr-NLS-GrLuc-ssrA	*LYS9pr-NLS-GrLuc-ssrA*	URA3
pNB763	p406-MET17pr-FLuc	*LYS9pr-FLuc*	URA3
pNB767	p406-SIC1pr-mCherry	*SIC1pr-FLuc*	URA3
pNB812	p405-RNR1pr-yEVenus	*RNR1pr-yEVenus-PEST*	LEU2
pNB813	p405-ACT1pr-yEVenus	*SIC1pr-yEVenus-PEST*	LEU2
pNB783	p406-MET17pr-FLuc	*RNR1pr-FLuc*	URA3
pNB785	p406-SIC1pr-mCherry	*SIC1pr-FLuc-yEVenus-PEST*	URA3
pNB789	p406-RNR1pr-FLuc	*RNR1pr-FLuc-yEVenus-PEST*	URA3

[a]Gene obtained by PCR. For details of source plasmid and oligos see Table 1.

TABLE 2: Plasmids.

Repression model

$$S(t) = S_{max} \quad \text{when } t < \delta$$

$$S(t) = S_{max}\exp[-(t-\delta)/\tau] + S_{min}\{1-\exp[-(t-\delta)/\tau]\} \quad \text{when } t > \delta$$

where S_{max} and S_{min} are the steady-state concentrations of induced and repressed luminescence signal, respectively. We used nonlinear least squares (nlinfit in MATLAB) to fit our repression model to average the luminescence signal of single cells repressed by the addition of metabolite. The best-fit curves are shown in Supplemental Figures S2–S6, with the corresponding best-fit parameters (and confidence intervals) shown in Supplemental Table S1. The same repression model and fitting procedure was used for fluorescence signal.

Strain	Genotype (relative to MMY116-2C)[a]	Gene integration
AMV104-02	*MET17pr-NLS-GrLuc-ssrA::URA3*	Multicopy
AMV68-10	*MET17pr-NLS-YeLuc-ssrA::URA3*	Multicopy
AMV69-06	*MET17pr-NLS-RdLuc-ssrA::URA3*	Multicopy
AMV45-06	*MET17pr-FLuc::URA3*	Multicopy
AMV152-03	*MET17pr-CBG99::URA3*	Multicopy
AMV151-08	*MET17pr-CBR::URA3*	Multicopy
AMV41-02	*MET17pr-NLS-NLuc::URA3*	Multicopy
AMV70-01	*MET17pr-NLS-GrLuc-ssrA::lys2Δ*	Single copy
AMV72-01	*MET17pr-NLS-YeLuc-ssrA::lys2Δ*	Single copy
AMV71-01	*MET17pr-NLS-RdLuc-ssrA::lys2Δ*	Single copy
AMV54-01	*MET17pr-FLuc::lys2Δ*	Single copy
AMV152-13	*MET17pr-CBG99::URA3*	Single copy[b]
AMV151-18	*MET17pr-CBR::URA3*	Single copy[b]
AMV16	*MET17pr-NLS-NLuc::lys2Δ*	Single copy
AMV50-08	*MET17pr-FLuc-yEVenus::URA3*	Multicopy
AMV63-03	*MET17pr-FLuc-yEVenus-PEST::URA3*	Multicopy
AMV141-08	*LEU2*[c] *LEU1pr-NLS-GrLuc-ssrA::URA3*	Multicopy
AMV150-18	*LEU2*[c] *LEU1pr-FLuc::URA3*	Multicopy
AMV153-17	*LEU2*[c] *LEU1pr-CBR::URA3*	Multicopy
AMV154-16	*LEU2*[c] *LEU1pr-CBG99::URA3*	Multicopy
AMV166-16	*LEU2*[c] *LEU1pr-FLuc-yEVenus*	Multicopy
AMV167-07	*LEU2*[c] *LEU1pr-FLuc-yEVenus-PEST*	Multicopy
AMV138-06	*ADE17pr-NLS-GrLuc-ssrA::URA3*	Multicopy
AMV148-04	*ADE17pr-FLuc::URA3*	Multicopy
AMV144-06	*LYS9pr-NLS-GrLuc-ssrA::URA3*	Multicopy
AMV149-15	*LYS9pr-FLuc::URA3*	Multicopy
AMV137-03	*SIC1pr-FLuc::URA3*	Multicopy
AMV156-04	*SIC1pr-yEVenus-PEST::LEU2*	Multicopy
AMV163-10	*SIC1pr-FLuc-yEVenus-PEST::URA3*	Multicopy
AMV155-12	*RNR1pr-FLuc::URA3*	Multicopy
AMV157-19	*RNR1pr-yEVenus-PEST::LEU2*	Multicopy
AMV165-12	*RNR1pr-FLuc-yEVenus-PEST::URA3*	Multicopy

[a]MATα can1-100 his3-11,15 trp1-1 leu2-3,112 ura3-1.
[b]Single-copy gene integration at URA3 locus was confirmed using PCR.
[c]LEU2 restored by integrating pRS405 plasmid into leu2-3,112 locus.

TABLE 3: Yeast strain genotypes.

Induction model

$$S(t) = S_{\min} \quad \text{when } t < \delta$$

$$S(t) = S_{\min} \exp[-(t-\delta)/\tau] + S_{\max}\{1 - \exp[-(t-\delta)/\tau]\} \quad \text{when } t > \delta$$

where S_{max} and S_{min} are the steady-state concentrations of induced and repressed luminescence signal, respectively. We used nonlinear least squares (nlinfit in MATLAB) to fit our induction model to average the luminescence signal of single cells induced by the removal of metabolite. The best-fit curves are shown in Supplemental Figures S2–S6. with the corresponding best–fit parameters (and confidence intervals) shown in Supplemental Table S1. The same induction model and fitting procedure was used for fluorescence signal.

Cell doubling time. We measured the doubling time of single cells before switching the medium at ~6 h by counting number of cells as a function of time. We used nonlinear least squares ("nlinfit" function in MATLAB) of a simple exponential $\exp[\ln_2(t/\lambda)]$ to fit the data. The estimated doubling time (λ) before medium switch and the 95% confidence intervals are shown in Supplemental Table S1. On average, cell-doubling time in medium with missing metabolites (SCD–Met, SCD–Leu, SCD–Ade, SCD–Lys) was ~93 min compared to ~86 min in complete medium.

ACKNOWLEDGMENTS

We are grateful to the Duke Center for Systems Biology for early seed funding, Akihiro Imai and Sam Johnson (Duke University, Durham, NC) for early help with luminescence microscopy, Carl Johnson (Vanderbilt University, Nashville, TN) for the FLuc plasmid, Megan Gray (Promega) for early access to NLuc, Ian Stanton (Duke University) for use of the Therien lab spectrophotometer, and Mats Kvarnström (Fraunhofer-Chalmers Centre, Göteborg, Sweden) for the CellStat image segmentation program. We thank Sam Johnson, Danny Lew, Stefano Di Talia, and the members of the Buchler lab for helpful comments on the manuscript. This work was funded by Defense Advanced Research Projects Agency Biochronicity Grant DARPA-BAA-11-66, National Institutes of Health Director's New Innovator Award DP2 OD008654-01, and Burroughs Wellcome Fund CASI Award BWF 1005769.01.

REFERENCES

Branchini BR, Magyar RA, Murtiashaw MH, Anderson SM, Helgerson LC, Zimmer M (1999). Site-directed mutagenesis of firefly luciferase active site amino acids: a proposed model for bioluminescence color. Biochemistry 38, 13223–13230.

Charvin G, Cross FR, Siggia ED (2008). A microfluidic device for temporally controlled gene expression and long-term fluorescent imaging in unperturbed dividing yeast cells. PLoS One 3, e1468.

Chiu CS, Kartalov E, Unger M, Quake S, Lester HA (2001). Single-molecule measurements calibrate green fluorescent protein surface densities on transparent beads for use with "knock-in" animals and other expression systems. J. Neurosci Methods 105, 55–63.

Di Talia S, Skotheim JM, Bean JM, Siggia ED, Cross FR (2007). The effects of molecular noise and size control on variability in the budding yeast cell cycle. Nature 448, 947–951.

Di Talia S, Wang H, Skotheim JM, Rosebrock AP, Futcher B, Cross FR (2009). Daughter-specific transcription factors regulate cell size control in budding yeast. PLoS Biol 7, e1000221.

Frydman J, Erdjument-Bromage H, Tempst P, Hartl FU (1999). Co-translational domain folding as the structural basis for the rapid de novo folding of firefly luciferase. Nat Struct Biol 6, 697–705.

Fujii H, Noda K, Asami Y, Kuroda A, Sakata M, Tokida A (2007). Increase in bioluminescence intensity of firefly luciferase using genetic modification. Anal Biochem 366, 131–136.

Garcia-Parajo MF, Segers-Nolten GMJ, Veerman JA, Greve J, Van Hulst NF (2000). Real-time light-driven dynamics of the fluorescence emission in single green fluorescent protein molecules. Proc Natl Acad Sci USA 97, 7237–7242.

Gedeon T, Bokes P (2012). Delayed protein synthesis reduces the correlation between mRNA and protein fluctuations. Biophys J 103, 377–385.

Grilly C, Stricker J, Pang WL, Bennett MR, Hasty J (2007). A synthetic gene network for tuning protein degradation in Saccharomyces cerevisiae. Mol Syst Biol 3, 127.

Hall MP, Unch J, Binkowski BF, Valley MP, Butler BL, Wood MG, Otto P, Zimmerman K, Vidugiris G, Machleidt T, *et al*. (2012). Engineered luciferase reporter from a deep sea shrimp utilizing a novel imidazopyrazinone substrate. ACS Chem Biol 7, 1848–1857.

Hoshino H, Nakajima Y, Ohmiya Y (2007). Luciferase-YFP fusion tag with enhanced emission for single-cell luminescence imaging. Nat Methods 4, 637–639.

Kvarnström M, Logg K, Diez A, Bodvard K, Käll M (2008). Image analysis algorithms for cell contour recognition in budding yeast. Opt Express 16, 12943–12957.

Kwon H, Enomoto T, Shimogawara M, Yasuda K, Nakajima Y, Ohmiya Y (2010). Bioluminescence imaging of dual gene expression at the single-cell level. BioTechniques 48, 460–462.

Leskinen P, Virta M, Karp M (2003). One-step measurement of firefly luciferase activity in yeast. Yeast 20, 1109–1113.

Liu AC, Welsh DK, Ko CH, Tran HG, Zhang EE, Priest AA, Buhr ED, Singer O, Meeker K, Verma IM, *et al*. (2007). Intercellular coupling confers robustness against mutations in the SCN circadian clock network. Cell 129, 605–616.

Loening AM, Fenn TD, Wu AM, Gambhir SS (2006). Consensus guided mutagenesis of Renilla luciferase yields enhanced stability and light output. Protein Eng Des Sel 19, 391–400.

Luker KE, Smith MCP, Luker GD, Gammon ST, Piwnica-Worms H, Piwnica-Worms D (2004). Kinetics of regulated protein-protein interactions revealed with firefly luciferase complementation imaging in cells and living animals. Proc Natl Acad Sci USA 101, 12288–12293.

Malleshaiah MK, Shahrezaei V, Swain PS, Michnick SW (2010). The scaffold protein Ste5 directly controls a switch-like mating decision in yeast. Nature 465, 101–105.

Mateus C, Avery SV (2000). Destabilized green fluorescent protein for monitoring dynamic changes in yeast gene expression with flow cytometry. Yeast 16, 1313–1323.

Mihalcescu I, Hsing W, Leibler S (2004). Resilient circadian oscillator revealed in individual cyanobacteria. Nature 430, 81–85.

Nakajima Y, Kimura T, Sugata K, Enomoto T, Asakawa A, Kubota H, Ikeda M, Ohmiya Y (2005). Multicolor luciferase assay system: one-step monitoring of multiple gene expressions with a single substrate. BioTechniques 38, 891–894.

Nakajima Y, Yamazaki T, Nishii S, Noguchi T, Hoshino H, Niwa K, Viviani VR, Ohmiya Y (2010). Enhanced beetle luciferase for high-resolution bioluminescence imaging. PLoS One 5, e10011.

Orr-Weaver TL, Szostak JW, Rothstein RJ (1981). Yeast transformation: a model system for the study of recombination. Proc Natl Acad Sci USA 78, 6354–6358.

Ozawa T, Kaihara A, Sato M, Tachihara K, Umezawa Y (2001). Split luciferase as an optical probe for detecting protein-protein interactions in mammalian cells based on protein splicing. Anal Chem 73, 2516–2521.

Robertson JB, Stowers CC, Boczko E, Johnson CH (2008). Real-time luminescence monitoring of cell-cycle and respiratory oscillations in yeast. Proc Natl Acad Sci USA 105, 17988–17993.

Sadowski I, Su T-C, Parent J (2007). Disintegrator vectors for single-copy yeast chromosomal integration. Yeast 24, 447–455.

Saito K, Chang Y-F, Horikawa K, Hatsugai N, Higuchi Y, Hashida M, Yoshida Y, Matsuda T, Arai Y, Nagai T (2012). Luminescent proteins for high-speed single-cell and whole-body imaging. Nature Commun 3, 1262.

Schindelin J, Arganda-Carreras I, Frise E, Kaynig V, Longair M, Pietzsch T, Preibisch S, Rueden C, Saalfeld S, Schmid B, *et al*. (2012). Fiji: an open-source platform for biological-image analysis. Nat Methods 9, 676–682.

Sheff MA, Thorn KS (2004). Optimized cassettes for fluorescent protein tagging in Saccharomyces cerevisiae. Yeast 21, 661–670.

Skotheim JM, Di Talia S, Siggia ED, Cross FR (2008). Positive feedback of G1 cyclins ensures coherent cell cycle entry. Nature 454, 291–296.

Spellman PT, Sherlock G, Zhang MQ, Iyer VR, Anders K, Eisen MB, Brown PO, Botstein D, Futcher B (1998). Comprehensive identification of cell cycle-regulated genes of the yeast Saccharomyces cerevisiae by microarray hybridization. Mol Biol Cell 9, 3273–3297.

Vieites JM, Navarro-García F, Pérez-Díaz R, Pla J, Nombela C (1994). Expression and in vivo determination of firefly luciferase as gene reporter in Saccharomyces cerevisiae. Yeast 10, 1321–1327.

Viviani VR, Bechara EJ, Ohmiya Y (1999a). Cloning, sequence analysis, and expression of active Phrixothrix railroad-worms luciferases: relationship between bioluminescence spectra and primary structures. Biochemistry 38, 8271–8279.

Viviani VR, Silva AC, Perez GL, Santelli RV, Bechara EJ, Reinach FC (1999b). Cloning and molecular characterization of the cDNA for the Brazilian larval click-beetle Pyrearinus termitilluminans luciferase. Photochem Photobiol 70, 254–260.

Wang X, Errede B, Elston TC (2008). Mathematical analysis and quantification of fluorescent proteins as transcriptional reporters. Biophys J 94, 2017–2026.

Wilson T, Hastings JW (1998). Bioluminescence. Annu Rev Cell Dev Biol 14, 197–230.

Wood KV, DeLuca M (1987). Photographic detection of luminescence in Escherichia coli containing the gene for firefly luciferase. Anal Biochem 161, 501–507.

Xu Y, Piston DW, Johnson CH (1999). A bioluminescence resonance energy transfer (BRET) system: Application to interacting circadian clock proteins. Proc Natl Acad Sci USA 96, 151–156.